RESEARCH ARTICLE OPEN ACCESS

Studies On The Dc Electric Field Effects On The Combustion Of Fuel Droplets

Solomon Benghan and Tryfon T. Charalampopoulos*
Combustion and Laser Diagnostics Laboratory,
Department of Mechanical Engineering, Louisiana State UniversityBaton Rouge, LA 70803, USA
Correspondingauthor: Solomon Benghan

ABSTRACT
The application of a DC electric field has been investigated as a method to improve the combustion efficiency of combustion devices in the face of a dire need to efficiently utilize our limited energy sources. Experimental studies have been carried out[1-4]to investigate the influence of an electric field on the combustion of a droplet.
In this study, the simplified burning droplet model is used to predict the droplet lifetime with and without an electric field. Comparisons are also made with different available models [5, 6] and the results assessed.
The electric force per unit volume exerted on neutral gas molecules is known to provide the convective effect, known as the "ionic wind", around the droplet in the presence of an electric field. Knowledge of the force distribution around the burning droplet may provide a better insight on the mechanisms and potentially improved control of the combustion of the droplet. Towards this end, different electrode configurations – plane, divergent and convergent – providing varying electric field have been explored.
The results suggest that the divergent electrode configuration yields the largest force per unit volume of the combustion gases.

Date of Submission:16-08-2018 Date of acceptance: 30-08-2018

I. INTRODUCTION

In 1814, Brande [7] reported that an electric field influences the heat and mass transfer between a candle flame and the electrodes; such that the flame itself and soot are drawn toward the negatively charged surface [3, 7]. There have also been recent investigations.

Ueda et al. [3] investigated experimentally the effect of a DC field on the combustion of a single droplet for sooting and non-sooting fuels. They observed that the reaction zone for the non-sooting fuel deformed towards the negative electrode. The luminous flames for the sooting fuels were mainly deformed towards the negative screen. Soot lumps emitted from flame gravitated to both positive and negative screens. The burning rate constant of fuels investigated increased with electric field strength. A maximum increase of 50% of its initial burning rate constant was recorded for the most sooting fuel investigated, Toluene. Increases in the burning rate constant under electric field was similar to that predicted using empirical equations from burning rate constant under forced convection conditions. For the most sooting fuel the additional increase in the burning rate constant was attributed to the reduction of radiative heat loss from reduction of emitted soot under an electric field condition [3].

Mikami and co-workers [8, 9], studied experimentally the interaction of two burning n-heptane fuel droplets under micro-gravity condition and showed that the droplet burning lifetime reaches a minimum value at a critical normalized droplet spacing, $(\ell / d_0)_{cr}$. Here ℓ denotes the distance between the centers of the support fibers of the two droplets and d_0 the initial droplet diameter. They attributed this minimum to the effects of radiative heating of the droplets. For$(\ell/d_0) < (\ell/d_0)_{cr}$, a single flame surrounded both droplets for most of the droplet lifetime, a situation referred to as the merged flame regime. While$(\ell/d_0) > (\ell/d_0)_{cr}$, individual flames surrounded each droplet, a situation called the separated-flame regime [8].

Okai et al. [4] extended Ueda's study to consider droplet interaction effects in an electric field. A pair of n-octane droplet of droplet diameter 0.70 mm ($\pm$0.05mm) with non-dimensional spacing ℓ/d_0 ranging between 2.67 and 15.4 was placed in an electric field of voltage drop 3.3 kV and an estimated maximum field of 55kV/m. They studied the effects of electric fields on droplet-pair burning in the merged-flame regime $(\ell/d_0) < (\ell/d_0)_{cr}$, with $\ell/d_0 = 2.67 - 3.08$; the transitional regime $(\ell/d_0) \approx (\ell/d_0)_{cr}$, with $\ell/d_0 = 9.33 - 10.8$; and the separated flame regime $(\ell/d_0) > (\ell/d_0)_{cr}$, with $\ell/d_0 = 13.3 - 15.4$. In the merged-flame regime, the field effects for droplet pairs resembled those for single droplets [4]; the effect of the field on the

burning-rate constant was comparable, and the flame shapes were similar, although elongated more symmetrically for the droplet pairs. In the transition flame regime, at a given time after ignition, increasing the field intensity promotes flame separation. In this regime, near the critical spacing, a merged flame exists until the middle of the burn, after which individual flames surround each droplet. As the electric field gradient, E, increases from zero, the flame gradually becomes more deformed, and for $E \geq 15\ kV/m$, individual flames surround each droplet throughout the entire burn. It was reported that the flame surrounding the droplet close to the negative electrode was visually similar to the flame surrounding a single droplet in a convective flow. The flame surrounding the droplet close to the positive electrode, however, was similar to that of a single quiescent droplet under microgravity in the same electric field [4]. In the separated regime, the droplet close to the negative electrode behaved similarly as observed in the transition regime. The flame around the droplet nearest the positive electrode, however, seemed more elongated towards the positive electrode, which suggested a predominance of negatively charged soot there. The burning rate constant in this regime was observed to be almost independent for droplet nearest to the positive electrode. The droplet closest to the negative electrode, however, exhibited obvious variation in the burning rate constant with the electric field strength. Okai et al. [4] attempted to explain their observations based on the assumption that the droplet closest to the negative electrode experienced electric wind, while the other droplet did not. Thus, the droplet close to the negative electrode was exposed to a convective velocity analogous to that experienced by a droplet in a forced flow or a single droplet in a large electric field. This convective flow reduced the residence time for soot formation thereby also reducing the degree of sooting. This was observed to be even more significant at the higher range of field intensities. The droplet nearest to the positive electrode not under the influence of an electric wind behaved more like a single droplet burning under a lower electric field. It sooted more strongly than the other droplet since it had larger residence times and exhibited a flame elongated in both directions. Okai et al. [4] concluded that the positive ions swept away from the flame of the droplet closest to the positive electrode formed the electric wind experienced by the droplet closest to the negative electrode.

NOMENCLATURE

DDiameter (m)
e Electronic charge (C)/ eccentricity of ellipse
eEccentricity of ellipse
EElectric field strength (V/m)
FForce/unit volume of gas
jCurrent density (A/m^2)
kThermal conductivity (W/m-K)
kIonic mobility (m^2/V-s)
KEvaporation constant (m^2/s)
Le Lewis number
mMass (kg)
$\dot{m}$Mass flow rate (kg/s)
nN umber of charge carriers
NuNusselt number
PrPrandtl number
rRadius (m)
r_0Radius of flame (m)
ReReynolds number
ShSherwood number
t_dDroplet lifetime (s)
TTemperature (K)
vVelocity (m/s)
v_r Radial velocity (m/s)
vWind velocity (m/s)
VElectrical potential (V)
x Distance between electrodes
y Distance between electrodes

Greek Symbols

εPermittivity (F/m)
ε_oPermittivity of free space (F/m)
ε_rRelative permittivity
γSecondary electron emission coefficient
ρ_lDensity of liquid (kg/m^3)
ρDensity (kg/m^3), charge density (C/m^3)
δ_M Film thickness based on mass
δ_T Film thickness based on heat

II. MODEL AND METHOD

The analysis of the combustion of a fuel droplet under an electric field was performed by first understanding the combustion of a single droplet without the presence of electric field. The approach was to use simple theoretical method, already developed, to predict the behavior of the droplet. The results are then compared with experimental data. Furthermore, the effect of an electric field will be included in the analyses and results also compared with similar published experimental results.

Godsave [28] recognizes two mechanisms as responsible for the reduction of size of a single droplet, low temperature evaporation and high temperature evaporation. The first mechanism occurs when the ambient temperature is aboutthe same as that of the fuel droplet. In this mechanism, evaporation rate is controlled by diffusion processes. The diffusion process is dependent on the vapor pressure of the liquid. The second mechanism occurs when there is a significant difference between the temperature of the droplet and the

ambient temperature. Here, the heat transfer from the ambient to the droplet determines the rate of evaporation.

If it is assumed that the evaporation rate of the fuel droplet under combustion is due to diffusion processes only, the evaporation rate of the fuel droplet can be analyzed using mass transfer principle. Similarly if pure heat transfer is assumed in the evaporation process, the fuel droplet can be analyzed using heat transfer principle. However it is known that the evaporation of a burning droplet depends on both heat transfer and mass transfer mechanisms. In order to show this physics, the mass transfer evaporation model, the heat transfer evaporation model and the simple burning droplet evaporation model as developed by Turns[5] are compared. The models used here were derived from solving the conservation equations (mass conservation, species mass conservation and energy conservation) with some assumptions – symmetrical droplet with a spherical diffusion flame around it is assumed; constant thermodynamics and physical properties is assumed; constant droplet surface temperature;stoichiometric reaction adopted; unity Lewis number is adopted in the simple burning droplet evaporation model and appropriate boundary conditions as recommended by Turns were also implemented. It should be pointed out that the Schvab-Zeldovich form of the energy equation with radiation effect included was what was being used.

In the presence of an electric field, the normal thermal trajectory paths of the ions generated in the flame and their velocities are altered; the ions gravitate towards the electrodes with charges opposite that which they possess. Consequently, the movement of the generated ions in the flame results in the movement of the neutral gas molecules surrounding the flame. This is due to the drag force induced on the molecules by the moving ions [10].The additional energy obtained by the ions from the field is lost to collision with neutral gas molecules. The collision could be either elastic or inelastic [11]. In this study, the effect the movement of the neutral gas molecules surrounding the flame is of concern.

As earlier stated, the fundamental effect the electric field induces is the change of the velocities and normal 'thermal' trajectories of the ions. This modification increases the velocity of the gases in the direction of the field [11]. When the collision is elastic, the extra momentum obtainedby the ions is conserved. It is this momentum that results toa body force acting on the gas [11]. It is reported that the effect of the force on the gas molecules is equally the same for both positively and negatively charged ions [12].

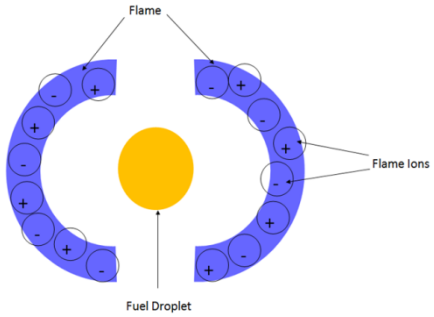

Figure1 (a) Burning fuel droplet just after ignition, before the application of an electric field

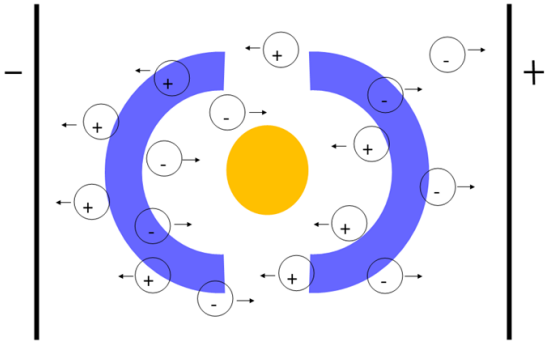

Figure 1 (b) Movement of the flame ions influenced by the presence of an applied electric field

The body force acting per unit volume of gas must be equal to the body force acting on the ions within it, assuming thatthe ions have attained equilibrium i.e. no acceleration of the ions [12].

$$F = Ee(n_+ - n_-), \quad (1)$$

Where F = force/unit volume of gas, $n_+$and$n_-$are the numbers of positive and negative charge carriers respectively, e is the charge of an electron and E is the local electric field strength. The above given body force only applies within the flame itself, in the thin reaction zone where charges of opposite polarity are generated and exist. The thin reaction region were charges of opposite polarity exist cannot contribute much to the body force on the gas. Much of the effect of the field is determined by occurrences between the flame and the electrode [11, 13]. Outside theflame, the space between the flame an the electrodes, thebody force acting per unit gas for a 1-dimensional system is given as [11]

$F_+ = Een_+$In the region between flame and negative electrode (2a)

$F_- = Een_-$In the region between flame and positive electrode (2b)

The value of E and n varies along the distance from the flame to the electrode. Gauss's law gives this variation and its relationship with the applied voltage [11],

$$\frac{dE}{dx} = -4\pi e(n_+ - n_-) = -\frac{d^2V}{dx^2} \quad (3)$$

Wherex is the perpendicular distance to the electrode and V is the applied voltage.

An important parameter in measuring the practical effect of the electric field on the flame is the number of ions flowing across a unit area parallel to the electrode, i.e. the current density. In the region between the flame and the electrode where no ion is generated, the current density must be constant at steady state [13],

$j = eE(n_+k_+)$In the region between the flame and the negative electrode (4a)

$j = eE(n_-k_-)$In the region between the flame and the negative electrode (4b)

Where k is the ionic mobility and the field is not greater than 3 x 10^4 V/cm times the pressure in atmospheres [12]. Substituting into equation 2 implies that,

$\pm F = j/k_{\pm}$ (5)

It is noted that the model for a simple burning droplet is applicable in a non-convective environment and stagnant environment i.e. no relative velocity between the droplet and the free stream, and no buoyancy [13]. With the application of an electric field, the resulting 'ionic wind' provides the needed convection for combustion of the fuel droplet. In incorporating convective effect, due to the ionic wind, into the simple burning droplet burning model, the chemical engineering film theory as recommended by Turns [5] is adopted. The film radii are given by

$$\frac{\delta_T}{r_s} = \frac{Nu}{Nu-2} \quad (6a)$$

$$\frac{\delta_M}{r_s} = \frac{Sh}{Sh-2} \quad (6b)$$

Where δ_T and δ_M are the film thickness based on heat and mass transfer respectively. They are defined in terms of the Nusselt number, Nu, and the Sherwood number, Sh. In physical terms, the Nusselt number is the dimensionless temperature gradient at the droplet surface and the Sherwood number is the dimensionless concentration (mass fraction) gradient at the surface. Faeth [14] synthesized a correlation which computes the Nusselt number at low and high Reynolds's numbers ($Re < 1800$)

$$Nu = 2 + \frac{0.555\ Re^{1/2}Pr^{1/3}}{[1+1.232/(RePr^{4/3})]^{1/2}} \quad (7)$$

The conservation equations are again solved analytically with modifications made to the inner and outer region of the simple burning droplet model, using the new defined film thicknesses; film thickness based on the heat and mass transfer. Appropriate modification to the initial boundary conditions of the burning droplet without the presence of an electric field are also made as proposed and shown by Turns [5]. Solutions are obtained for the mass burning rate, droplet evaporation rate, temperature profile for the inner and the outer region.

Mathematically, the difference in the solution (mass burning rate, radius of flame, temperature profiles)solving the conservation equation in the absence of an electric field when compared to the solution in the presence of an electric field is the appearance of the Nusselt and Sherwwod number. These numbers capture the effect of the externally applied electric field on the combustion of the fuel droplet, modifying the temperature profile of the inner and outer region of the fuel droplet, the mass burning rate of the fuel droplet and the flame radius. In obtaining the droplet life time plots, a correction factor recommended by Sioui [15] was introduced.

Figure 2 shows the variation of the squared droplet diameter with time without the presence of an electric field.Yamashita[2] reported a burning rate constant of 0.597mm^2/s. 14.910mm^2/s, 1.380mm^2/s and 0.612mm^2/s were observed for the heat model, mass transfer model and simple burning droplet model respectively. There was a very good agreement of the simple burning model with Yamashita's experiment.

The variation of the squared droplet diameter with time under an electric field of 4.5KV/cm is shown in Figure 3. Experimental and simulation result from Yamashita are compared with the simple droplet burning model. As expected the droplet diameter decreases with time. 0.602mm^2/s, 0.532mm^2/s and 0.724mm^2/s are the burning rate of Yamashita's experimental, Yamashita's simulation and the simple burning droplet model respectively. Thevariation in the burning rate constants can be due to some of the assumptions adopted.

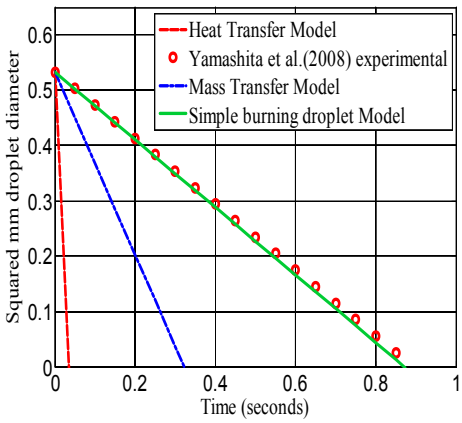

Figure 2 Time history of squared droplet diameter. Heat transfer evaporation model, Mass transfer evaporation model and simple burning droplet model compared with experimental result from Yamashita et al.[2]

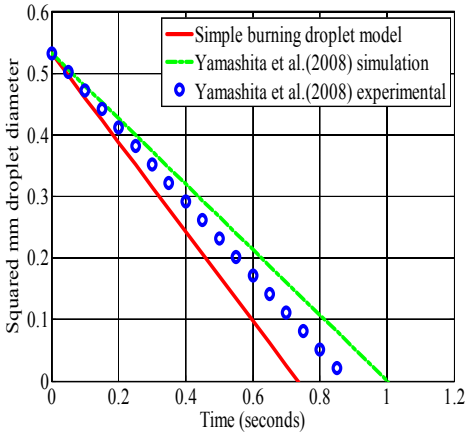

Figure 3 Time history of squared droplet diameter under an electric field of 4.5KV/cm. Simple droplet burning model compared with experimental and simulation result from Yamashita et al.[2]

Figure 4 (a.) and Figure 4 (b.), compares the variation of the temperature in the inner and outer region respectively of the burning droplet with and without the presence of an electric field. In the inner region, the presence of the electric field shrinks the radius of the region while the maximum temperature, flame temperature, was approximately the same.The temperature variation in the outer region follows the same trend as with and without an electric field.

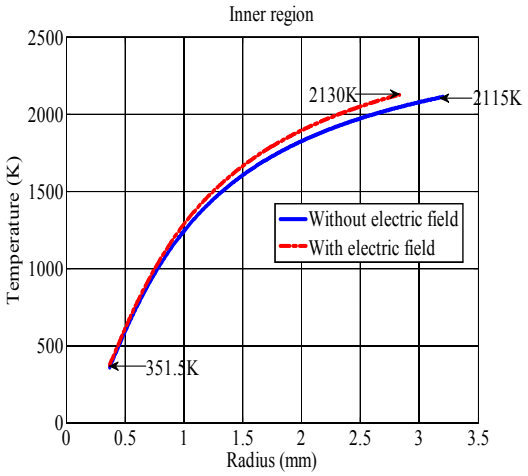

Figure 4 (a.) Temperature profile of the inner region of the simple burning droplet model with and without an electric field compared.

However, due to ionic wind induced by the electric field, the convective heat loss to the ambient occurs more rapidly compared to that detected when an electric field is absent. Consequently, the lower temperature observed when an electric field is applied.

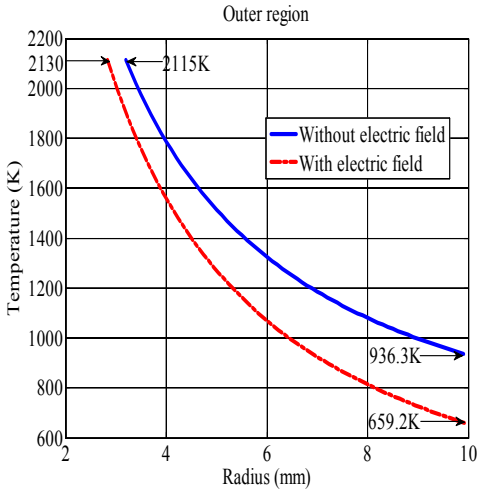

Figure 4 (b.) Temperature profile of the outer region of the simple burning droplet model with and without an electric field compared.

Electrode Configuration

Having established the fact that an electric field influences

the combustion physics of a burning fuel droplet, the studies proceed to examine the influence of a modified electrode on the combustion of the fuel droplet. In the past, most investigation on the effect of electric field on flame and combustion has been based on plane parallel electrode geometry with the flame sandwiched in between them. Accurate physical measurement of the electric field has been reported[16, 17] to be problematic, as the measuring probe modifies the electric field. Hence no clear justification for this configuration has been found. In this work, different electrode configurations are examined. The electric field produced by these configurations and their possible effect on the magnitude of the ionic wind velocity is compared and assessed.

Furthermore, the equation for the magnitude of the ionic wind generated for some electrode configurations has been reported[12, 13], which is discussed later. When the magnitude of the wind velocity is known, the Reynolds number of the flow can be determined. Thus the effect on combustion can be predicted by the appropriate modification of the relevant equation with the convective effect due to the ionic wind.

By examining the reported wind velocity equation (stated later), it is observed that the magnitude of the velocity is dependent on the value of the current density, j, with the other factors usually constant. The value of the current density is dependent on [12]:

a. The finite rate of generation of ion in the flame zone
b. Space charge in the electrode region, and is largely independent of the ion source

Not much can be done to modify a., the finite rate of ion generation in the flame, since it is a flame parameter. The second determining factor occurs when the field becomes so large (values vary with flames) that ion energies are sufficient to cause secondary collision with other species. This consequently reduces the wind velocity in two ways:

I. The secondary ions tend to neutralize those from the reaction zone
II. Loss of energy of ions in other forms other than momentum

To maximize current density, within safe limits i.e. avoiding secondary ionization and electric field breakdown, divergence of the electric field lines is explored. This can be achieved by geometric modification of the electrodes. Figure 5, shows the electrode configurations studied. Figure 5 (a.) is the prevalent plane parallel electrode configuration. Figure 5 (b.) and figure 5 (c.) are a divergent electrode and a convergent electrode.

As mentioned earlier, not so much advancement has been made in modeling the electric field in the presence a flame due to the complexities involved in the analysis. The coupling of the flame and the electric field requires a combination of computational fluid dynamics, a chemical kinetics mechanism which includes ions and an electric field modeling program[18]. Yamashita et al. [2], Pederson et al. [19] and Papac et al. [20] have done some work in developing one. However, they still fall short of predicting the exact amount of ions generated in the flame and their location. Due to this complexity in the modeling of electric field in the presence of flame, the field in the absence of flame is modeled for this study. Gauss's law in S.I. unit gives the electric field between electrodes, arising from a potential difference between them and the space charge distribution between them.

$$\nabla \cdot E = \frac{\rho}{\varepsilon} \quad (8a)$$

$$\varepsilon = \varepsilon_0 \varepsilon_r \quad (8b)$$

Where$\nabla$is the del operator used to express the divergence of a vector; E is the electric field strength; ρ is the charge density; ε is the permittivity which is a product of the permittivity of free space, $\varepsilon_0 = 8.854 \times 10^{-12}\ \mathrm{F.m^{-1}}$, and the relative permittivity, ε_r.

$$E = \nabla V \quad (9)$$

WhereV is the electric potential, this is substituted into the equation to give the Poisson's equation,

$$\nabla^2 V = \frac{\rho}{\varepsilon} \quad (10)$$

Electric field was modeled using COMSOL[21]. Since the electric field is to be modeled in the absence of flame, the charge density, ρ, is assumed to be zero thus reducing the Poisson equation, equation to a Laplace equation, equation.

$$\nabla^2 V = 0 \quad (11)$$

COMSOL[21] solves the Laplacian equation for the electric potential using finite element method. The electric field and flux is then computed. The models are created in 2-D with the electrodes kept 6cm apart, comparable to what has been observed in literature. The electrodes are kept at 10kV and -10kV. 10kV is just an arbitrary voltage choice, expected to produce a field below breakdown voltage, 30kV/m. Space between electrode is assumed to be filled with air, hence the relative permittivity, $\varepsilon_r = 1$.

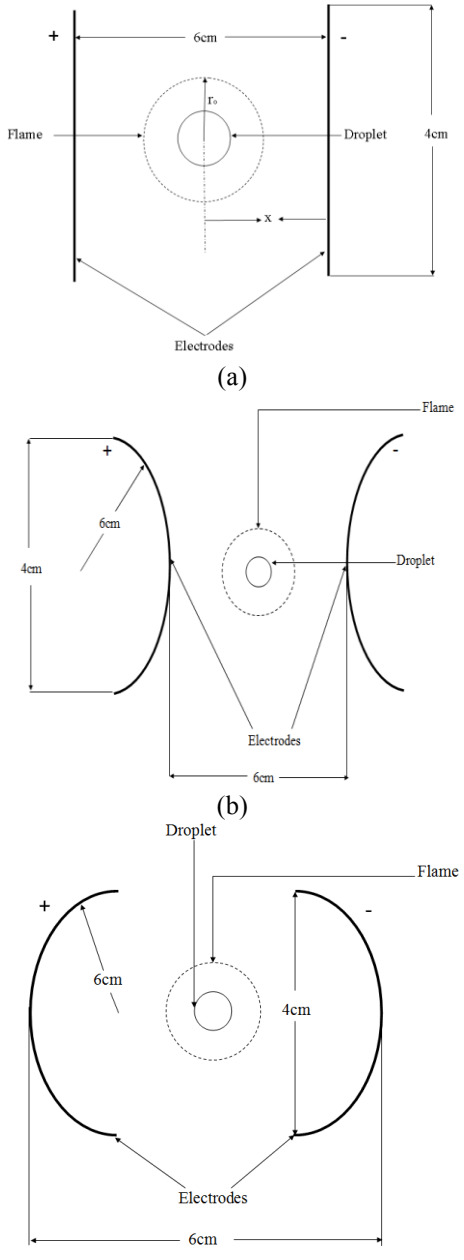

Figure 5 Schematic of electrode configurations (a) Plane electrodes (b) Divergent electrodes (c) Convergent electrodes.

For the configurations (1-dimensional) shown in Figure 5, Weinberg and Payne [12, 13] gave the ionic wind velocity at the electrode as

$$v = \pm \left[\frac{jx}{k_{\pm}\rho}\right]^{0.5} \quad (12)$$

where v is the wind velocity; x is the distance between the electrode and the flame; j is the current density; k is the ionic mobility and ρ is the density of the gas.

Figure 6 illustrates the variation of the electric field strength in the y-axis at the mid-distance between the electrodes, placed at 10kV and -10kV potential respectively. The electric field strength is strongest at the midpoint of the cross-sectional distance where there appears to be the maximum number of field lines running through. The plane electrode configuration showed the highest field strength at this location (where the droplet for investigation is likely to be positioned, since it exposes the droplet to a balanced field effect from both electrodes at opposite potential). The strength of the plane electrode varied from 2.58kV/cm – 3.10kV/cm compared to 1.19kV/cm – 2.34kV/cm (divergent electrode) and 1.64kV/cm – 3.05kV/cm (convergent electrode), thus providing a more uniform electric field.

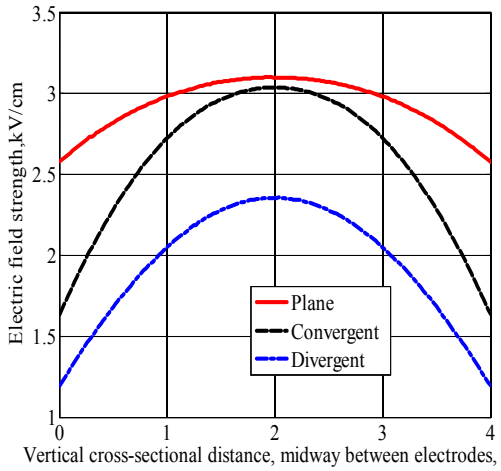

Figure 6 Variation of the electric field (Equation 9) across the cross-section (y-axis) of the parallel area mid-distance between the electrodes for different configurations – plane, convergent and divergent.

Figure 7 shows the variation of the electric field with x-axis, distance from one electrode to the other. From theory, the electric field strength is inversely proportional todistance. Hence the field strength tends to decrease away from the location of the charged electrodes. The plane electrode showed maximum field strength (3.59kV/cm) at the plates and then decreases gradually to a minimum (3.10kV/cm) midway between the electrodes. The divergent electrode follows a similar trend to that of the plane electrode but with a much steeper gradient – strongest field strength of 5.27kV/cm at the electrodes and the weakest field (2.34kV/cm) at mid distance between both electrodes. The strong field reported at the divergent electrode is due to the

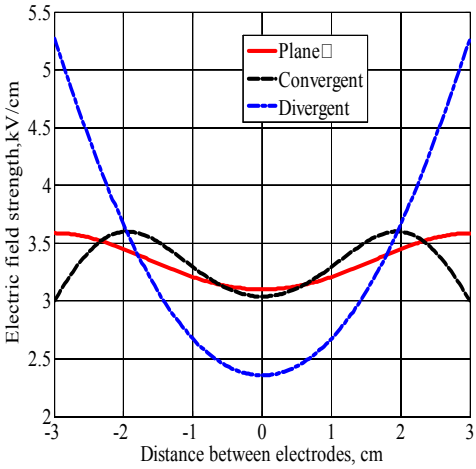

Figure 7 Variation of the electric field (Equation 9) with distance (x-axis) between the electrodes for different configurations – plane, convergent and divergent.

concentration of electric field lines as a result of the geometry of the electrode. At midway between the divergent electrodes, the field decreases to a minimum as expected from theory and further decreases due to lower electric field line concentration. This is because the electric field lines are diverged away as a result of the geometry of the electrode. The convergent electrode shows a somewhat different profile. It increases from the electrode to a maximum (3.60kV/cm) about a centimeter away from the electrode and then decreases gradually to a minimum (3.04kV/cm) at the mid-distance between the electrodes. The maximum field strength experienced about a centimeter away from the electrode is due to concentration of electric field lines as a result of the curvature of the electrode – the curvature of the electrodes focuses the electric field lines. Comparing these – electrodes, the plane electrode provides a more uniform electric field and the strongest magnitude of electric field at the likely location of the fuel droplet.

The variation of the current density with distance from electrodes is shown in Figure 8. As expected, the current density follows a similar trend as the electric field strength. Higher current densities were observed at sites were the electric field strength was stronger and lower current densities at the corresponding weaker field locations.

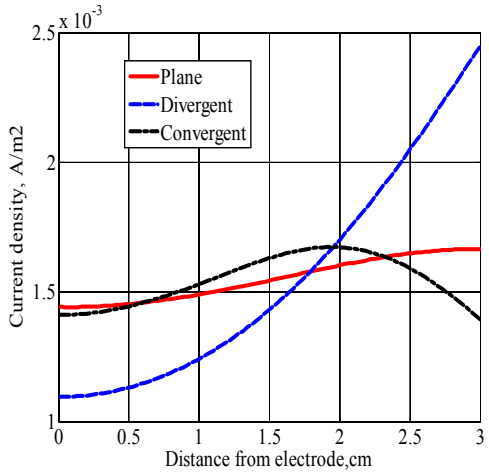

Figure 8 Current density (Equation 4a.) profiles with distances from the electrode for different configurations – plane, convergent and divergent.

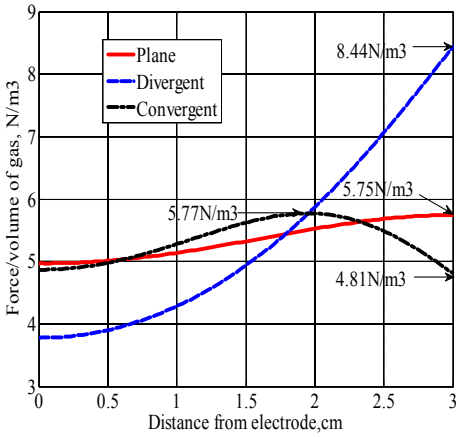

Figu**re 9** Magnitude of body force acting per unit gas with location along the x-axis.

The variation of the magnitude of the body force per unit volume of gas with distance from electrode is plotted in Figure 9. The similarity in the trend of figure 8 and figure 9 is as a result of the dependence of the body force per unit volume of unit gas on the current density. It is this force that drives the ionic wind responsible for the convective effect present in the combustion of a droplet in the presence of an electric field.

Figure 10 illustrates the variation of the magnitude of the ionic wind velocities with distance from the electrodes for the different electrode configurations. It is known that the magnitude of the ionic wind is dependent on both the magnitude of the current densities and the aerodynamic property (i.e. the geometry) of the electrode configuration.

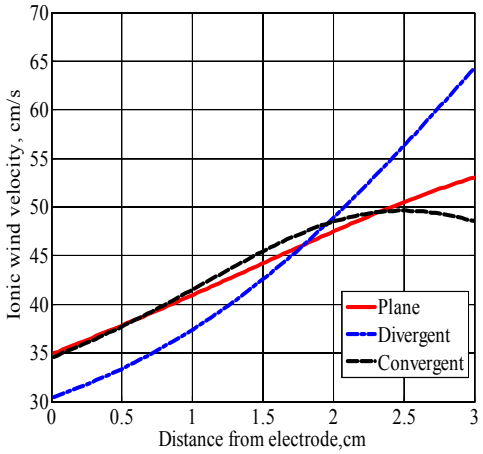

Figure 10 Magnitude of Ionic wind velocities (Equation 12) compared for different electrode configuration – Plane, convergent and divergent.

The ionic wind velocities increase with electric field from the location of the assumed ion source, at mid-distance between electrodes, to the electrode surface, for the plane, convergent and divergent electrode configurations. This is so because as the electric field strength increases, the drift velocities of the ions increases, consequently leading to more elastic collisions with neutral gas molecules in the path of the ions.

SUMMARY

In this study, the influence of an electric field on the combustion of fuel droplets was investigated. The objective was to gain better understanding of the combustion of fuel droplets and the physics behind the effect of anapplied electric field on the combustion of fuel droplets and to improve the combustion efficiency of fuel droplets by the application of such a field. Furthermore, the effect of various electrode configurations on the electric field was also investigated. The findings of this study are as follows:

1. Heat transfer evaporation model, mass transfer evaporation and a simple burning droplet evaporation model was studied. These models were used to analyze a stationary ethanol droplet of 0.73mm diameter. The time droplet lifetime profile was plotted and compared with result from a similar experimental work. Yamashita reported a burning rate constant of $0.597mm^2/s$. $14.910mm^2/s$, $1.380mm^2/s$ and $0.612mm^2/s$ were observed for the heat transfer evaporation model, mass transfer evaporation model and simple burning droplet model respectively. The results clearly show that the mass transfer evaporation model and the heat transfer evaporation model do not entirely capture the physics of the burning droplet. On

the other hand, the simple burning droplet model was in good agreement with the experimental result.

2. Having established the validity of the simple burning droplet model, an electric field of 4.5kV/cm was applied around the stationary ethanol fuel droplet. The double film theory adopted in developing the simple burning droplet model was modified using the Nusselt number and the Sherwood number to define a new radii for the inner and the outer region. This was done to capture the convective effect from the developing ionic wind. The result showed an increment in the burning rate constant of the ethanol droplet from 0.612mm^2/s in the absence of an electric field to 0.724mm^2/s i.e. an 18.3% increment in the burning rate constant of the ethanol droplet. However, the result compared to experimental and simulation work done by Yamashita shows some disparity – the disparity maybe due to changing ambient conditions. Also, the assumption of constant surface temperature of the burning droplet could be a factor.
3. The parallel plane electrode configuration has been widely used in similar works in the past without any clear validation for their preference. Modified configurations- divergent and convergent electrode configuration was looked at. It was found that although the plane electrode does not produce the strongest field strength value, it produced a more consistent and uniform electric field around the space where the droplet is located, which is desired. This may explain its use in experiments reported in literature. Nevertheless, it is not evident that a uniform electric field around the droplet leads to more improved combustion, and hence higher fuel efficiency.
4. In order to gain insight into the pattern of the convective effect providing the ionic wind around a burning droplet in the presence of an electric field, the force per unit volume acting on the neutral gas molecules providing this influence was plotted (figure 9) for the different electrode configurations investigated. The largest magnitude of force per unit volume of gas computed for these electrodes were given as follows: divergent electrode – 8.44 x 10^{-6} N/cm^3, convergent electrode – 5.77 x 10^{-6} N/cm^3 and the plane electrode – 5.75 x 10^{-6} N/cm^3.

In the light of limited experimental work done in this area, more experimental studies are required to gain even more in depth knowledge about the physics of this problem. Furthermore, most of the studies (experimental and theoretical) available in literature so far have been focused on electric field from DC current. It would be useful to investigate the effect of the field from an AC current on the combustion of fuel droplets.

It is known that NO_x formation thrives at high temperature. As reported in this work, a lower temperature profile (Figure 4 (b.)) was observed at the outer region of the burning droplet when an electric field was applied. An in depth study needs to be carried to explore the possibility of reducing NO_x formation via the application of an electric field.

To our knowledge, no experimental work has been done on the effect of modifying the electrode configurations. Experimental work is suggested to validate some of the results obtained from the electrode modification analyses performed in this study.

Furthermore, the effects of higher ionic winds velocities attained with divergent configuration (Figure 10) merit further scrutiny.

REFERENCES

[1]. Imamura, O., et al., Combustion of ethanol fuel droplet in vertical direct current electric field. Proceedings of the Combustion Institute, 2011. **33**(2): p. 2005-2011.
[2]. Yamashita, K., et al., Influences of Uniform Electrical Fields on Burning Rate Constant of Ethanol Droplet Combustion. Combustion Science and Technology, 2008. **180**(4): p. 652-673.
[3]. Ueda, T., et al., Combustion behavior of single droplets for sooting and non-sooting fuels in direct current electric fields under microgravity. Proceedings of the Combustion Institute, 2002. **29**(2): p. 2595-2601.
[4]. Okai, K., et al., Effects of DC electric fields on combustion of octane droplet pairs in microgravity. Combustion and Flame, 2004. **136**(3): p. 390-393.
[5]. Turns, S.R., An Introduction to Combustion: Concepts and Applications. 2000: McGraw-Hill Higher Education.
[6]. Kuo, K.K., Principles of combustion. 1986: Wiley.
[7]. Brande, W.T., The Bakerian Lecture: On Some New Electro-Chemical Phenomena. Proceedings of the Royal Society of London, 1814.
[8]. Mikami, M., et al., Interactive combustion of two droplets in microgravity. Symposium (International) on Combustion, 1994. **25**(1): p. 431-438.
[9]. Lawton, J., P.J. Mayo, and F.J. Weinberg, Electrical Control of Gas Flows in Combustion Processes. Proceedings of the Royal Society of London. Series A. Mathematical and Physical Sciences, 1968. **303**(1474): p. 275-298.

[10]. F. B. Carleton, F.J.W., Electric field induced flame convection in the absence of gravity. Nature, 1987. **330**.
[11]. K. G. Payne, F.J.W., A Preliminary Investigation of Field-Induced Ion Movement in Flame Gases and Its Applications. Proceedings of the Royal Society of London. Series A. Mathematical and Physical Sciences, 1959. **250**(1262): p. 316-336.
[12]. Weinberg, J.L.a.F.J., Maximum Ion Currents from Flames and the Maximum Practical Effects of Applied Electric Fields. Proceedings of the Royal Society of London. Series A. Mathematical and Physical Sciences, 1964. **277**(1371): p. 468 - 497.
[13]. Payne, K.G. and F.J. Weinberg, Mesurements on field-induced ion flows from plane flames. Symposium (International) on Combustion, 1962. **8**: p. 207-217.
[14]. Faeth, G.M., Current Status Of Droplet And Liquid Combustion. Progress in Energy and Combustion Science, 1977. **3**: p. 191 - 224.
[15]. Sioui, R.H. and L.H.S. Roblee Jr, The prediction of the burning constants of suspended hydrocarbon fuel droplets. Combustion and Flame, 1969. **13**(5): p. 447-454.
[16]. Franjo Cecelja, M.B., and Wamadeva Balachandran, Lithium Niobate Sensor for Measurement of DC Electric Fields. IEEE Transactions on Instrumentation and Measurement, 2001. **50**(2): p. 465-469.
[17]. Lawton, J. and F.J. Weinberg, Electrical aspects of combustion. 1969: Clarendon P.
[18]. Dolmansley, T.J.C., C.W. Wilson, and D.A. Stone, Electrical Modification of Combustion and the Affect of Electrode Geometry on the Field Produced. Modelling and Simulation in Engineering, 2011. **2011**: p. 1-13.
[19]. Pedersen, T. and R.C. Brown, Simulation of electric field effects in premixed methane flames. Combustion and Flame, 1993. **94**(4): p. 433-448.
[20]. Papac, M.J. and D. Dunn-Rankin, Modelling electric field driven convection in small combustion plasmas and surrounding gases. Combustion Theory and Modelling, 2007. **12**(1): p. 23-44.
[21]. COMSOL Multiphysics, in Modeling Guide. 2007, COMSOL AB, http://comsol.com.
[22]. Glassman, I. Combustion, 3rd Ed., Academic Press, San Diego,CA,1996.

Solomon Benghan "Studies On The Dc Electric Field Effects On The Combustion Of Fuel Droplets "'International Journal of Engineering Research and Applications (IJERA) , vol. 8, no.8, 2018, pp 35-44